LiT: Fine-grained Toothbrushing Monitoring with Commercial LED Toothbrush

Kaixin Chen[1], Lei Wang[1], Yongzhi Huang[2,3], Lu Wang[1,*], Kaishun Wu[2,3]
[1]CSSE, Shenzhen University, China, [2]Hong Kong University of Science and Technology, China,
[3]Hong Kong University of Science and Technology (Guangzhou), China
{2017133035,2018132012,huangyongzhi}@email.szu.edu.cn,wanglu@szu.edu.cn,wuks@ust.hk

ABSTRACT

Neglecting proper oral hygiene has proven to potentially lead to severe oral disease, resulting in complications over time. Careful brushing can mitigate the problem, but it is common for individuals to dedicate insufficient time to the various areas of their teeth. We propose LiT to monitor the brushing situation of 16 Bass technique surfaces in real-time. LiT relies on commercial toothbrushes with blue LEDs as a transmitter and requires only 2 low-cost photosensors as receivers on the toothbrush head. However, the transmission channel of light in the oral cavity is unclear. Finding the optimal deployment positions and minimizing the number of photosensors is challenging. To tackle these obstacles, we design the positioning of the 2 photosensors and create a transmission model within the oral cavity to verify the feasibility theoretically. Additionally, obstacles in implementation include separating brushing action accurately, interference of light on the outer surfaces of front teeth, and individual variability. To overcome these challenges, we develop corresponding technologies and a comprehensive framework. Experiments with 16 users show that LiT achieves a highly accurate recognition rate of 95.3% with an error estimate for brushing duration of 6.1%. Furthermore, LiT also proves resilient under user motion and environmental interference.

CCS CONCEPTS

• **Human-centered computing** → **Mobile computing**; **Ubiquitous and mobile computing systems and tools**; • **Applied computing** → *Physics*; • **Computer systems organization** → **Embedded and cyber-physical systems**; • **Hardware** → **Sensor applications and deployments**.

KEYWORDS

Oral health; Toothbrushing monitoring; Visible light channel modeling; Visible light sensing; Blue light

ACM Reference Format:
Kaixin Chen[1], Lei Wang[1], Yongzhi Huang[2,3], Lu Wang[1,*], Kaishun Wu[2,3]. 2023. LiT: Fine-grained Toothbrushing Monitoring with Commercial LED Toothbrush. In *The 29th Annual International Conference on Mobile Computing and Networking (ACM MobiCom '23), October 2–6, 2023, Madrid, Spain.* ACM, New York, NY, USA, 16 pages. https://doi.org/10.1145/3570361.3613287

1 INTRODUCTION

Motivation: Oral diseases like caries and gum disease caused by poor oral hygiene are prevalent worldwide, and affect people from all age groups [1]. Furthermore, poor oral hygiene can catalyze various other diseases, including respiratory, digestive, arthritis, cardiovascular, and kidney disease [2]. Pathogenic bacteria in dental plaque are the primary cause of these diseases [3, 4]. Fortunately, brushing teeth carefully in the proper duration can reduce plaque and prevent oral diseases [5]. Nonetheless, the time spent by ordinary people brushing on different tooth surfaces is uneven, which leads to severe negative impacts on oral health [1, 6–10]. For example, people spend more time brushing the visible vestibule and occlusal surface, and less time on the inner and outer surfaces of the molars or even miss them [6, 7]. Insufficient brushing can lead to plaque accumulation on some tooth surfaces, while excessive brushing can cause damage to gums and enamel in certain areas. Both scenarios can lead to costly oral diseases and complications over time [1, 8–11].

Hence, to enhance the users' tooth-cleaning benefit and efficiency, various methods for monitoring tooth brushing have been proposed, including using cameras, microphones, inertial sensors, and magnetic sensors. Although camera-based methods [12–14] can determine the orientation of a toothbrush through external cameras, they are expensive and impractical to use, especially in low-light conditions and

*Lu Wang is the corresponding author.

ACM MobiCom '23, October 2–6, 2023, Madrid, Spain

ACM ISBN 978-1-4503-9990-6/23/10…$15.00
https://doi.org/10.1145/3570361.3613287

raise privacy concerns. Similarly, microphone-based methods [15–17] are limited in their recognition accuracy and are adversely affected by environmental noise. Inertial sensor-based methods [6, 18–20] face accuracy decline from accumulated drift errors and struggle with user motion and vibrations. Magnetic sensor-based methods [19, 21] are inconvenient to deploy and are affected by electromagnetic interference and user motion. Overall, these methods are limited by high costs, impractical deployment, low accuracy, and poor robustness. Therefore, addressing these shortcomings in toothbrushing is necessary to meet commercialization.

Our Approach: Can a *low-cost, easy-to-deploy* sensing paradigm be used for *robust* and *highly accurate* toothbrushing monitoring across various environments and motion conditions? Due to the uniqueness of each oral cavity area, a more sophisticated lidar would have the capability to track and monitor the precise location of the toothbrush within the oral cavity. The blue LED lighting increasingly found in toothbrushes for bacterial control [22–24] gives us this opportunity. Because the transmission and reflection of LED light are distinct due to variations in the mouth's structure, a well-placed photosensor would do well to implement this lidar. As shown in Figure 5, we propose LiT, which adds two low-cost photosensors to the toothbrush head to monitor the brushing through the dynamic light intensity change. LiT is robust since it shields ambient interference, such as light, sound, and electromagnetic fields, and the user's motion interference, such as moving and turning the head. Moreover, it is low-cost and easy to deploy, which is much more accurate than external sensors like cameras, magnetic sensors, inertial sensors, and microphones.

Challenges and Solution: Although the proposal seems promising, implementing this concept into an actionable system should overcome a series of obstacles, such as: *(i)* Firstly, the transmission channel of light in the oral cavity is unclear. The optimal deployment positions and minimizing the photosensors are significant challenges. We analyzed the Bass technique's characteristics, the oral cavity's structure, and the toothbrush head's luminous properties to determine the deployment positions of the two sensors. A light transmission model was established to verify the feasibility theoretically. *(ii)* Secondly, the overabundant intensity light can hinder distinguishing the users' brushing action if we only use the photosensors. We found a unique character in the brushing signal with stable periodicity and symmetry to overcome this challenge. This allows us to identify and segment the brushing motion accurately. *(iii)* Thirdly, brushing the outer surfaces of the front teeth can be disturbed by strong ambient light. We separated this particular case from the signal and proposed a compression formula to eliminate the interference. *(iv)* Fourth, individual variability among users produces signal fluctuation. We extracted stable relationship features between 2 sensor signals to counter instability and amplify the discrimination of the brushing surfaces.

Summary of Experiment Results: In our evaluation with 16 participants, LiT demonstrated an average recognition accuracy of 95.3% for 16 Bass technique surfaces, with an estimated error of brushing duration of 6.1%. The training model exhibited cross-user versatility and temporal stability. More importantly, LiT overcomes the robustness of current brushing monitoring systems. It can be used for both manual and electric toothbrushes and maintains robust performance under various light conditions and user motion.

Contributions: We first propose using toothbrush light for monitoring brushing, extending light-sensing use case to brushing monitoring. Compared with existing paradigms, our method has the advantage of shielding from environmental interference and user motion. Then, we build a model of light propagation in the mouth to reveal the working principle and theoretical feasibility. Next, we propose a brushing signal segmentation algorithm, ambient light interference cancellation technology, and feature extraction technology to ensure time-accurate and accurate brushing monitoring. At last, we deployed LiT and evaluated on 16 users. The results show LiT has good brushing monitoring capabilities, cross-user versatility, and temporal stability. LiT can also be used for manual and electric toothbrushes and maintains strong performance under various experimental conditions.

2 RELATED WORK

In this section, we review the related literature of LiT.

Oral health approaches. The mobile computing community has presented mobile health methods related to oral health to improve oral health behaviors, such as guiding users with short messages [25, 26], integrating correct brushing posture guiding into the intelligent mirror [27], using the game-based feedback mechanisms [13, 14, 28], checking and detecting oral diseases by taking photos from smartphones [29, 30], provide health notifications [31, 32], providing dental plaques number feedback [33], and using social interaction to motivate users [34].

Toothbrushing monitoring. [19] and [21] respectively use the magnetic sensor in the wristband or on the wall to capture the magnetic field generated by the toothbrush's built-in magnet and the vibration motor to achieve tooth brushing monitoring. Still, they are inconvenient to deploy and vulnerable to user motion and electromagnetic interference. Playful Toothbrush [12] uses the camera in front of the user to recognize the special pattern of the toothbrush handle. Face tracking is added to reduce false positives further [14]. However, vision-based methods are relatively expensive and inconvenient to deploy. Moreover, they cannot be used in weak light and may cause privacy concerns

[35]. The microphone of the mobile phone [17] and headset [15, 16, 36] can be used to distinguish brushing areas. But microphones can be easily disturbed by noise and cannot be used with electric toothbrushes [21]. Some studies embedded inertial sensors in toothbrush handles [18], while others leverage smartwatch inertial sensors for brushing monitoring [6, 19, 20]. However, the accumulation of drift errors negatively impacts accuracy [37], especially under the influence of user motion and electric toothbrush vibration [21]. In general, the existing methods suffer from limitations: high cost, requirement of additional equipment, low accuracy, and poor robustness against environmental and user motion factors. In contrast, LiT overcomes these limitations. LiT only requires the integration of two low-cost photosensors on the toothbrush head without the need for additional equipment. Moreover, LiT's sensors are positioned inside the mouth during brushing, which not only keeps the sensors relatively stable to the user's mouth regardless of how the user moves, but also shields ambient light interference. Our innovative intraoral perception approach is unique compared to prior methods that involve sensors outside the mouth.

Light perception. Light, as an electromagnetic wave, is not only used for communication [38–41], but it also plays a crucial role in ubiquitous sensing. The ceiling lamp after encoding spatial information can be utilized for indoor positioning [42–44] and human sensing [45, 46]. The attenuation of light in air and the reflection and absorption of light by the hand are used for gesture recognition [47–49], finger tracking [50, 51] and identity authentication [52]. The unique absorption spectra of different substances are used for wine monitoring [53, 54] and food recognition [55, 56]. Because the contraction and expansion of blood vessels affect the absorption of green light by blood, green light is also used to measure pulse [57], blood oxygen concentration [58], blood pressure [59, 60] and even identity authentication [61, 62]. In contrast, we first explored the feasibility of using light for low-cost tooth brushing monitoring and designed and developed systems with high accuracy and robust performance.

3 BASICS AND HARDWARE DESIGN

3.1 Bass Technique

The Bass technique, recommended by the American Dental Association (ADA), divides the teeth into 16 surfaces, including inner, outer, and occlusal surfaces (Figure 1), for proper cleaning [63, 64]. Brush strokes, depicted in Figure 2, are categorized into up-and-down and back-and-forth motions. To clean the inner and outer surfaces of front teeth and molars, position the toothbrush at a 45° and use gentle up-and-down strokes (tooth-wide). For molars' occlusal surfaces, employ back-and-forth strokes [65, 66]. Note that strokes should be parallel to the toothbrush for the inner surfaces of front teeth and molars' occlusal surfaces, and perpendicular for other cases.

3.2 Structure of Oral Cavity

According to Figure 3, the oral cavity comprises various structures, including lips, cheeks, palate, tongue, gingiva, and teeth. The front teeth are horizontally arranged at the front of the oral cavity, while the molars are perpendicular to the front teeth and situated behind them. The outer surfaces of the front teeth are connected to the gingiva and covered by the inner lip. The outer surfaces of the molars are connected to the gingiva and surrounded by cheeks. The inner surfaces of the upper teeth are connected to the palate, while the inner surfaces of the lower teeth are connected to the gingiva and attached to the tongue. The occlusal surfaces of the molar are perpendicular to the inner and outer surfaces. Notably, the upper teeth are wider than the lower teeth, approximately half the width of the molar (5mm). Through preliminary analysis, it was found that the spatial characteristics of front teeth and molars, inner and outer surfaces, occlusal surfaces, and upper and lower teeth are distinctive. Nevertheless, the characteristics of the left and right molars do not demonstrate a substantial difference. For instance, the outer surfaces of the left and right molars are covered by the cheeks.

3.3 Toothbrush Head Luminous Properties

Commercially available blue light toothbrushes deployed 2 to 4 blue light LEDs at the base of the bristles of the toothbrush head. LEDs' light is emitted from the surface of the bristles after being reflected and transmitted (refracted) by the bristles. Since the light emitted from the bristles is close to the reflective surfaces (e.g., teeth and gum) during brushing, it cannot be considered as parallel light. We treat the light emitted from the bristles as a collection of point sources (top and curved surface of an elliptical cylinder). As the reflection and refraction inside the bristles are difficult to model, we observed the luminous properties experimentally. As shown in Figure 4(a), the photosensor was placed very close to the bristle surface (3mm) in a parallel position in the dark environment, and the entire bristle surface's luminous properties were collected by constantly moving the photosensor. As shown in Figure 4(b), we found that the intensity distribution of the point source on the top and curved surface was relatively uniform. Moreover, the light intensity of the point light source on the top (4661–10693 lux) was significantly greater than that on the curved surface (1210–1576 lux) due to less blockage by the bristles. However, when brushing, the top of the bristles are always against the teeth, so the point light from the top is blocked. Therefore, the toothbrush light source can be simplified to a set of point light sources with uniform light intensity on the curved surface of an elliptic

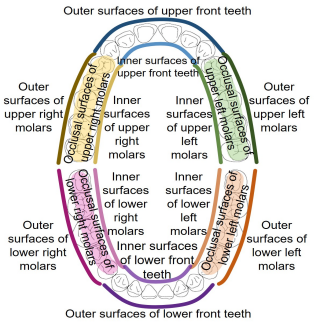

Fig. 1. 16 Bass technique surfaces.

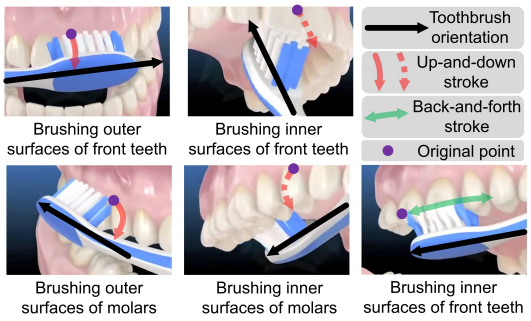

Fig. 2. Bass technique (showing how the teeth are brushed).

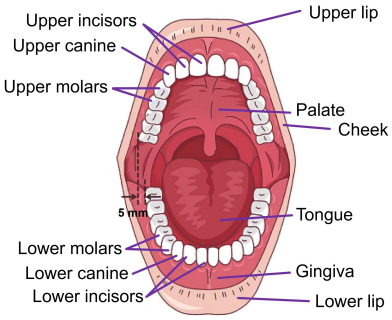

Fig. 3. Structure of the oral cavity.

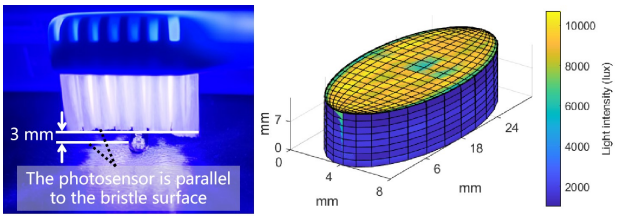

Fig. 4. (a) Measurement experiment setup. (b) Luminous properties of the bristles.

cylinder. We evaluated 5 different toothbrushes in Section 7.5 and obtained a consistent conclusion.

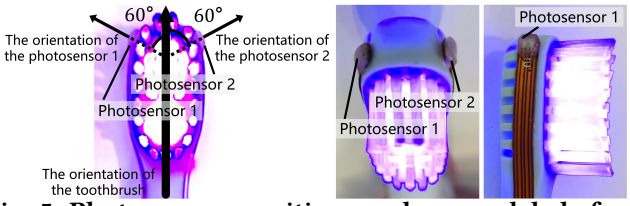

Fig. 5. Photosensors positions and sensor labels for each view.

3.4 Hardware Design

3.4.1 Consideration of Photosensor Deployment Position. Our goal is to optimize sensor placement to showcase the characteristics of Bass technology and oral cavity structure in the received signal. After careful consideration and extensive experimental tests, we deployed two photosensors at the side of the toothbrush, near the top, and at approximately 60° from the toothbrush orientation, as depicted in Figure 5. We thoroughly analyze all the factors of this issue.

(i) Combined with Section 3.3 (luminous properties), as shown in Figure 6(a), the sensor faces away from the luminous surface to block direct light. The sensor should also maintain a shorter travel distance to ensure a stronger reflection of light. If the photosensor is deployed on the front of the toothbrush (Figure 6(b)), more light will directly enter the photosensor, which may overwhelm the reflected light-containing features. If the photosensor is deployed on the back of the toothbrush (Figure 6(c)), only a tiny amount of light can barely enter the response angle of the sensor.

(ii) According to Section 3.1, there are two situations between the stroke direction and the toothbrush orientation, that is, parallel or vertical. As shown in Figure 7, our sensor orientation can receives signal changes in both directions. Note that the change of light intensity perpendicular to the toothbrush orientation significantly impacts the total signal intensity because of a smaller angle between them.

(iii) From Section 3.2, there is no obvious feature difference between the left and right molars. However, when brushing the left and right molars, the rolling angle of the toothbrush is exactly the opposite (Figure 8). We deployed the sensors on either side of the toothbrush. Using the asymmetry of the two sensor signals, we can distinguish left and right molars.

3.4.2 Hardware Design Details. We used the Texas Instruments OPT3002 ($0.581) as the photosensor with a range of 300nm–1000nm. Figure 9 is the LiT circuit diagram. The ADDR pins of the two photosensors were connected to the GND and VCC pins of the Arduino, respectively, to assign different addresses. The decoupling capacitor of $0.1\mu F$ kept the supply voltage stable. To facilitate the sensors' deployment on the toothbrush's side, we designed two long flexible PCBs (223.1 mm×3.8 mm×0.7 mm) and glued them to the toothbrush using silicone rubber. The sensor's surface was covered with a layer of about 0.6mm transparent food-grade silicone rubber, which prevented saliva from short-circuiting the sensor and ensured excellent light transmittance. After 86 hours of moisture curing in an environment with approximately 62% humidity, the system passed the short-time immersion test (IPX7 waterproof standard). The sampling rate was preset at 10Hz to ensure low power consumption.

4 CHANNEL MODEL OF BLUE LIGHT IN ORAL CAVITY

In this section, the channel model of blue light in the mouth is derived to introduce the working principle, and the theoretical feasibility is demonstrated by numerical simulation.

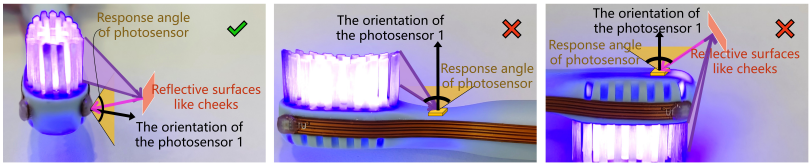

Fig. 6. Light channel diagram of the photosensor deployed on (a) the side, (b) the front, and (c) the back of the toothbrush.

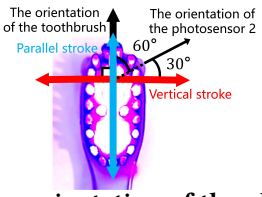

Fig. 7. The orientation of the photosensor intersects both 2 strokes.

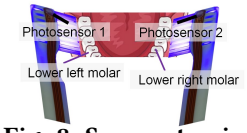

Fig. 8. Symmetry in the oral cavity.

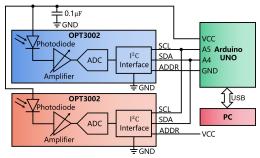

Fig. 9. Circuit diagram of LiT.

4.1 Single Light Channel Model

As shown in Figure 10(a), a beam of light is emitted from the light source point L on the toothbrush surface, propagated to the reflection point R (e.g., the tooth surfaces), and then received by the sensor S. The propagation process includes four parts of attenuation: the propagation loss from L to R is λ_{LR}, the surface loss at the reflection point R is λ_R, the propagation loss from R to S is λ_{RS}, and the reception loss at sensor S is λ_S. We believe that all reflections in the mouth are diffuse reflections. Therefore, according to Lambert's law [67], the reflected light intensity is proportional to the cosine of the angle between the normal of the reflecting surface and the incident light source, that is, $\lambda_R \propto \cos\theta_1$ and $\lambda_R \propto \cos\theta_2$. Moreover, The attenuation of light propagation through the air follows the inverse square law [68], that is, $\lambda_{LR} = \frac{1}{d_1^2}$ and $\lambda_{RS} = \frac{1}{d_2^2}$. Therefore, the intensity of a single beam of light received by receiver S can be expressed as:

$$I_S = I_L \cdot c \cdot \lambda_{LR} \cdot \lambda_R \cdot \lambda_{RS} \cdot \lambda_S = I_L \cdot c \cdot \frac{\cos\theta_1}{d_1^2} \cdot \frac{\cos\theta_2}{d_2^2} \quad (1)$$

where I_L is the light intensity of L. c is the reflectivity of S.

4.2 Dynamic Light Intensity Function

Take brushing the outer surfaces of the upper molars as an example. We first prove that we can only analyze the section shown in Figure 10(c) to simplify the calculation. As shown in Figure 10(b), a spherical coordinate system is established with the L as the origin, where the y-axis is parallel to the toothbrush and the z-axis is perpendicular to the gingival surface. Consider 2 reflection points A and B on the same horizontal line on the gingiva, where A, L, and S are on the xOz plane, and B is not on the xOy plane. $\langle\overrightarrow{LA}, \overrightarrow{Oz}\rangle = \theta_0$ and $\langle\overrightarrow{LA}, \overrightarrow{LB}\rangle = \alpha$. Since the angle between $\overrightarrow{LA}$ and $\overrightarrow{LB}$ is not large, we assume that A and B are on a spherical circle perpendicular to the z-axis, that is, $\langle\overrightarrow{LB}, \overrightarrow{Oz}\rangle = \theta_0$. Because the normal vectors of A and B are parallel to the z-axis, $\cos\langle\overrightarrow{AL}, \overrightarrow{n}\rangle = \cos\langle\overrightarrow{BL}, \overrightarrow{n}\rangle = \cos\theta_0$. On the other hand, $d_{LB} = \frac{d_{LA}}{\cos\alpha}$ and I_L and c are constants. Therefore, $I_{LB} = I_L \cdot c \cdot \frac{\cos\theta_1}{(\frac{d_{LA}}{\cos\alpha})^2} = I_{LA}\cos^2\alpha$. In the same way, $I_{BS} = I_{AS}\cos^2\alpha$ can be proved. Therefore, $I_{LBS} = I_{LAS}\cos^4\alpha$. During the process of rotating the toothbrush, the angle α between the point on the same horizontal line and A remains almost unchanged. Therefore, the reflected light intensity on the same horizontal line can be expressed as $k \cdot I_{LAS}$, where k is a constant coefficient.

Brushing is done by rotating the brush head around the handle and making short strokes. As shown in Figure 10(d), we took the toothbrush head as the origin of the coordinate system, and focused on the impact of the change of the rotation angle θ. The width of the toothbrush h and the distance between the toothbrush and the tooth a are regarded as constants, so $S(x, y) = (h\cos\theta, h\sin\theta)$, $L(x_1, y_1) = (\frac{y_1}{tan\theta}, y_1)$ and $R(x_2, y_2) = (a, y_2)$ and light intensity received by S can be written as the formula about θ, y_1, y_2:

$$\begin{aligned} I_S(\theta, y_1, y_2) &= I_L \cdot c \cdot \frac{\cos\theta_1}{d_1^2} \cdot \frac{\cos\theta_2}{d_2^2} \\ &= I_L \cdot c \cdot \frac{\sin\theta(a - \frac{y_1}{\tan\theta})(a - h\sin\theta) + \cos\theta(a - \frac{y_1}{\tan\theta})(y_2 - h\cos\theta)}{[(a - \frac{y_1}{\tan\theta})^2 + (y_2 - y_1)^2]^{\frac{3}{2}} \cdot [(a - h\sin\theta)^2 + (y_2 - h\cos\theta)^2]^{\frac{3}{2}}} \end{aligned} \quad (2)$$

By integrating the gingival plane (y2) where the reflection point is located and the toothbrush luminous surface (y1) where the light emitting point is located, the reflected light intensity of the gingival surface to the toothbrush luminous surface can be obtained:

$$I_{S_{gingiva}}(\theta) = \iint I_S(\theta, y_1, y_2)\, dy_1\, dy_2 \quad (3)$$

Finally, sum the reflected light intensity of multiple reflecting surfaces to get the received total light intensity:

$$I_{S_{sum}}(\theta) = \sum_{n=1}^{N} I_{S_{surface}}(\theta) \quad (4)$$

where N is the number of reflecting surfaces. As shown in Figure 10(e), the value of N can be different. The rotation angle θ of the toothbrush is related to the brushing time t, so the light intensity function is a dynamic function $I_{S_{sum}}(\theta(t))$ related to time t. Note that we only consider the effect of the single reflected light on the sensor because the exponential propagation attenuation has been significantly attenuated to negligible after multiple reflections.

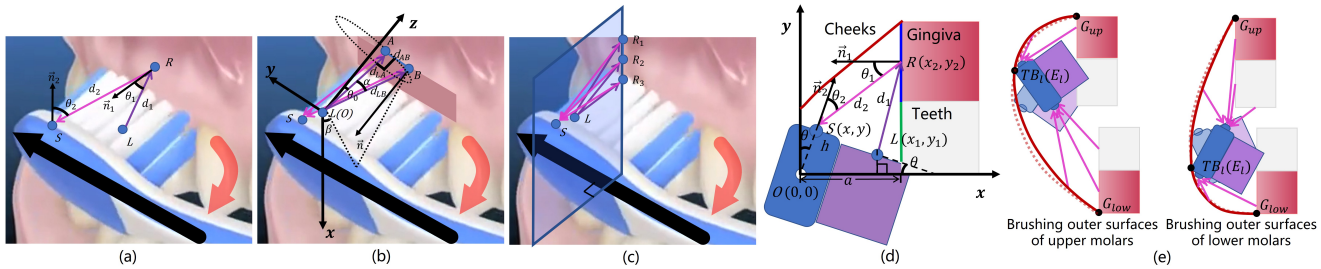

Fig. 10. (a) Single light channel model. (b) Spherical coordinate system with L as the origin. (c) Section perpendicular to the toothbrush. (d) Cross-section of reflected light. (e) The number of reflective surfaces is different when brushing different surfaces.

4.3 Numerical Simulation Results

We assume that the height and width of teeth and gums were both 1cm, and the upper molar protruded outward by 0.25cm. When brushing, there was a 1cm gap between the upper and lower molars. As shown in Figure 10(e), the curve of the cheek was a partial elliptical curve that passes through the boundary points G_{up} and G_{low} of the upper and lower gums, and the toothbrush's leftmost point TB_l. Plus, the elliptical curve's leftmost point E_l and TB_l coincided. Brushing speed was uniform. The reflectivity of gum, tooth, and cheek were set as 0.25, 1, and 0.1, respectively. We used Matlab to calculate the brushing signals for the 2 surfaces shown in Figure 10(e). The simulation results (Figure 11) show that the signals are still very different even when brushing the structurally similar outer surfaces of the upper and lower molars. Specifically, when brushing the outer surface of the lower molars and rotating the toothbrush upwards, there is an angle at which the upper sensor (sensor 1) receives the strongest reflection of the occlusal surface of the upper molars, causing a sudden increase in signal amplitude (Figure 11 (b)). However, when brushing the upper molars, the lower sensor (sensor 2) signal does not undergo a sudden increase.

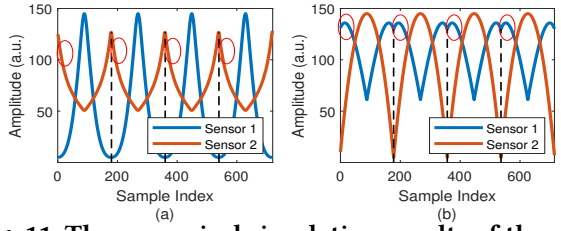

Fig. 11. The numerical simulation results of the outer surfaces of the (a) upper and (b) lower molars.

5 MEASUREMENT AND ANALYSIS

This section analyzes the signals collected under the influence of different factors, as the basis for the system design.

5.1 Effect of Vibration

The first question is whether LiT can be used for manual toothbrushes and electric toothbrushes. With the LEDs of the toothbrush turned on, a user placed the toothbrush on the occlusal surfaces of the lower left molars without brushing. Figure 12 shows the light intensity signals received by the 2 sensors before and after opening the vibration. We found that the vibration did not cause obvious fluctuation at the preset 10Hz sampling rate. This is because the vibration of the electric toothbrush belongs to high-frequency vibration (more than 20,000 times per minute [69]) and its amplitude is small. The low sampling rate of 10Hz automatically filters out high-frequency vibration noise.

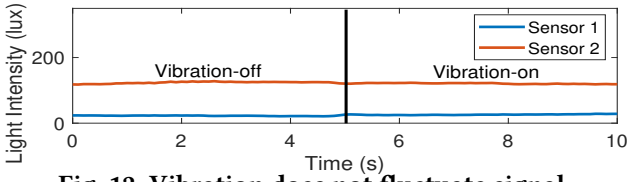

Fig. 12. Vibration does not fluctuate signal.

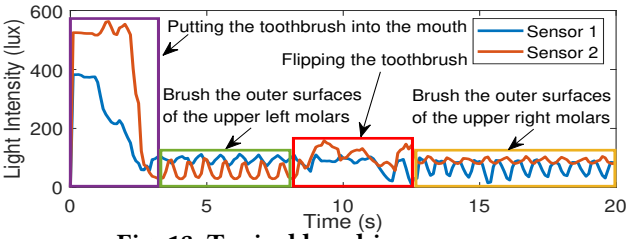

Fig. 13. Typical brushing process.

5.2 Characteristics of Brushing

Figure 13 shows a user's brushing process under the ceiling light. During the process of putting the toothbrush into the mouth, the 2 sensors receive ambient light with very high light intensity. When brushing the outer surfaces of the upper left molars, the signals of 2 sensors become stable. When the brushing surfaces are switched by turning the toothbrush, the light signals fluctuate again. The non-brushing period may produce greater light intensity, so we cannot utilize the light intensity to segment the brushing signal. However, the brushing process is repetitive, which is reflected in the periodic change of light intensity (Figure 14(a)). This periodicity allows us to distinguish between brushing and non-brushing.

Moreover, when we carefully amplify the signal, we can be surprised to observe the symmetry in a brushing cycle (Figure 14(b)). This is because the toothbrush needs to return to the original position (e.g., the root of the tooth (Figure 2)) along the original path after each stroke. This symmetry makes the brushing signal more characteristic and can help improve the time accuracy of segmentation.

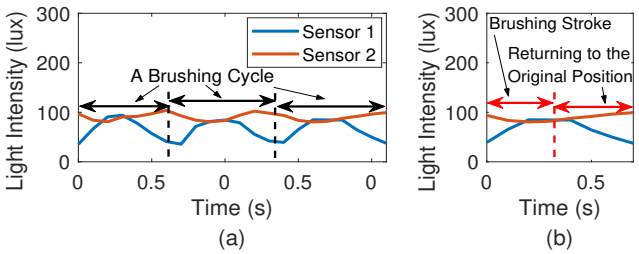

Fig. 14. (a) Periodicity and (b) symmetry of brushing signals on the outer surfaces of the upper right molars.

5.3 Effect of Ambient Light

We study how the environment variable most likely to cause interference (i.e., ambient light) affects the signal. We collected a user's brushing signals of 16 Bass technique surfaces under the ceiling light without turning on the toothbrush LEDs. We found that the light intensity received by 2 sensors was very weak (<8 lux) when brushing 14 Bass technique surfaces except for the outer surfaces of the front teeth. Figure 15 shows this observation. Our insight is: When brushing 14 Bass technique surfaces except for the outer surfaces of the front teeth, the sensors are located at the top of the toothbrush, in the oral cavity, and face the inside of the mouth. The direction of ambient light entering the oral cavity is also from the mouth to the inside, and is weak, which is partially blocked by oral tissues. After reflecting within the oral cavity, the light reaching the top sensor of the toothbrush becomes weaker in intensity. However, we noticed that the signals were strong when brushing the outer surfaces of the upper and lower front teeth because the sensors were not in the oral cavity and were only partially occluded by the lips (Figure 15(right)). Therefore, we further observed the brushing signals when the toothbrush LEDs were turned on under different light conditions (Figure 16). We found that the ambient light significantly affected the sensor facing toward the ceiling (Sensor 2). The maximum and amplitude of the signals increased with the increase in light intensity, but their minimum and waveform did not change significantly. Modulating the toothbrush LEDs at a frequency independent of ambient light and filtering the ambient light using FFT is a potential method, but it requires additional oscillator hardware and may need a higher sampling rate. In Section 6.2, we propose a technique to eliminate ambient light interference without extra hardware and a higher sampling rate.

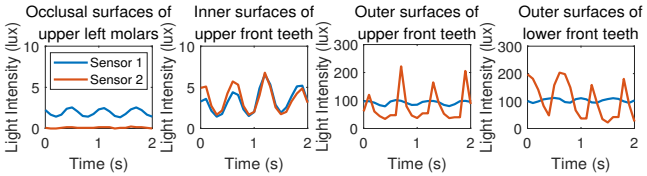

Fig. 15. The brushing signals when the toothbrush LEDs were turned off under the ceiling light.

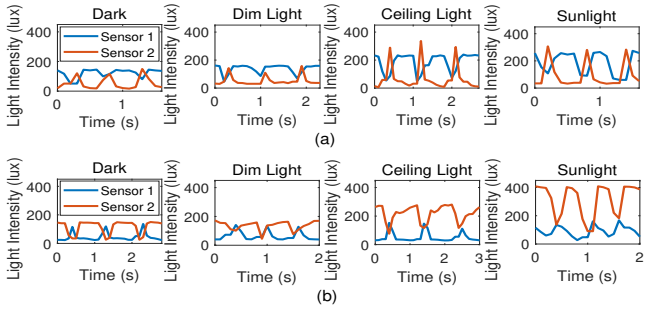

Fig. 16. Signals on the outer surfaces of (a) upper and (b) lower front teeth with varied lighting conditions.

5.4 Effect of Toothpaste

Figure 17 shows the user's brushing signals when using low-foam toothpaste (Zendium^{TM} toothpaste) and not using toothpaste. We found that the original brushing signals were consistent regardless of whether the toothpaste was used or not, which means that the low-foam toothpaste hardly affected the signals. Because the low-foam toothpaste produces less-dense foam after being dissolved by saliva, it does not extensively cover the reflective surfaces in the oral cavity (teeth, gums, etc.) [33]. Moreover, a small amount of foam covering the sensors' surfaces does not significantly attenuate light entering the sensors.

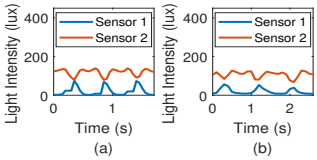

Fig. 17. The original brushing signals remained consistent whether (b) using toothpaste or (a) not.

5.5 Signal of 16 Bass Technique Surfaces

This section studies the signal difference of different Bass technique surfaces. A user sat in a dark room and brushed each of the 16 surfaces 10 times using low-foam toothpaste. We separately calculated the euclidean distance between each brushing cycle and other brushing cycles for each sensor signal. Then, we added the results of the 2 sensor signals and averaged all the cycles as a result. Note that to ensure the alignment of each brushing cycle, we performed piecewise linear interpolation for the 2 sensor signals collected. The result (Figure 18) shows that the intragroup euclidean

distance of each brushing surface is smaller than its inter-group distance, which also verifies the previous analysis and effectiveness of the hardware design.

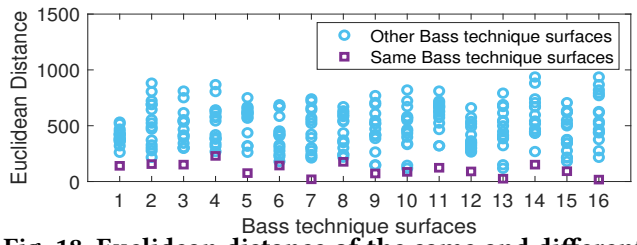

Fig. 18. Euclidean distance of the same and different Bass technique surfaces.

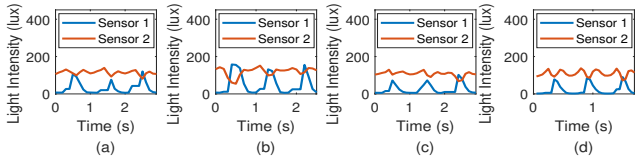

Fig. 19. Three brushing cycle signals of four users when brushing the outer surfaces of the lower left molars.

5.6 User Variability

Although dentists encourage users to use the standardized Bass technique, the differences between users include the brushing speed, uneven teeth and gums, mouth opening size, and changes in the position and inclination between the toothbrush and teeth, which produce signal variability. Figure 19 shows the brushing signals of 4 users on the outer surfaces of the lower left molars. We found that the variability is mainly reflected in the slight difference in duration and amplitude. We extracted the stable relationship features between the 2 sensor signals closely related to the brushing surfaces to counter this instability and amplify the differentiation of the brushing surfaces.

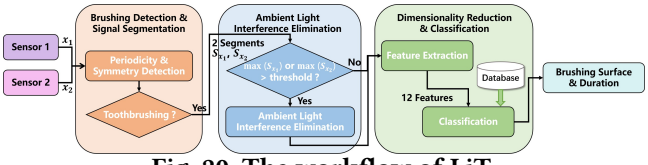

Fig. 20. The workflow of LiT.

6 FRAMEWORK

Figure 20 illustrates LiT's workflow. LiT first receives 2 photosensors' signals as input and determines whether it is a brushing action based on the periodicity and symmetry of the signals and segments the brushing signals. LiT then uses ambient light interference cancellation technology to eliminate the ambient light interference. Finally, the features of the signal segments are extracted and given to the classifier.

6.1 Brushing Signal Segmentation

The first task of LiT is to accurately segment the brushing signal in time. In Section 5.2, we found that periodicity and symmetry of signals are two necessary conditions for toothbrushing activity. First, we calculate the autocorrelation of 2 sensor signals within a window size of 27 (approximately 3 toothbrushing cycles). The autocorrelation of a signal is the correlation between the current signal and a signal that lags behind at a certain time. We first normalize the sensor signals to facilitate subsequent threshold judgment. Figures 21(b) and (c) are lag plots corresponding to Figure 21(a), showing the relationship between correlation and lag. We can see that autocorrelation has several large positive peaks and small negative valleys. The position of the negative valley indicates that the signal starting from this point has a completely negative correlation with the original signal. This negative correlation is due to the symmetry of the signals in the first and second half cycles of a toothbrushing cycle, which is a completely negative correlation. A large peak value indicates that the signal starting from this point has a completely positive correlation with the original signal, which also means the occurrence of a toothbrushing cycle. In contrast, if an aperiodic signal appears, it disrupts the characteristics of negative and positive alternating of the signal autocorrelation (Figure 22).

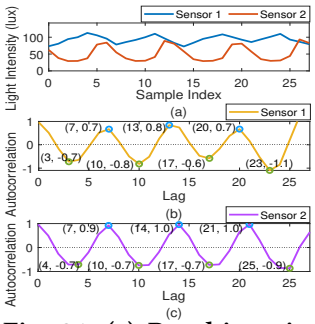

Fig. 21. (a) Brushing signals. (b) (c) autocorrelation of signals.

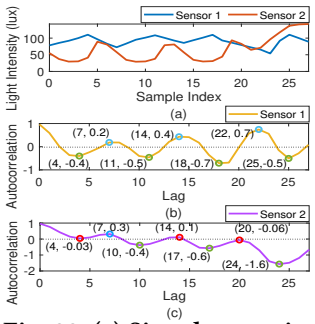

Fig. 22. (a) Signals containing non-brushing. (b) (c) autocorrelation of signals.

Therefore, when we simultaneously detect negative valleys and positive peaks that appear successively in the autocorrelation of 2 sensor signals, with both peaks>0.15 and valleys<-0.15, it is considered that the signals within the current window are periodic. Next, we slide the window and repeat the above operation. The step length is the length of the first toothbrushing cycle in the window. Note that there may be a deviation in the positive peak position of the autocorrelation between the 2 sensor signals. We select the peak position with greater autocorrelation to segment the signal. Figure 23 is an automatic segmentation result of Figure 13, indicating that our algorithm is robust in recognizing toothbrushing signals and segmenting each cycle of

the toothbrushing signal. Note that our algorithm only has a lag of 2.7 s at the beginning due to the need to fill the data of window size. In the subsequent judgment, the time interval is a toothbrushing cycle, which is < 1 s.

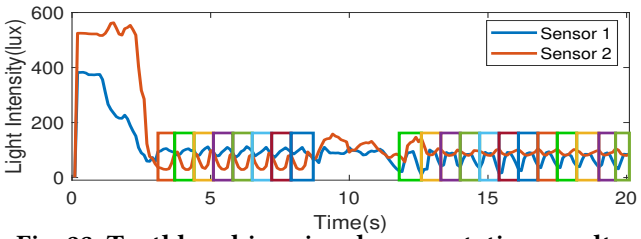

Fig. 23. Toothbrushing signal segmentation results.

6.2 Ambient Light Interference Cancellation

We conducted experiments in 10 rooms with ceiling lights on, allowing for comfortable visibility. These rooms varied in size, types of ceiling lights, quantity, and arrangement. We found that ambient light interferes the brushing signals on the outer surfaces of the front teeth, all reaching a maximum of more than 250 lux. This may be because enough light intensity ensures comfortable lighting. However, the brushing signals on the other 14 tooth surfaces were not affected and did not exceed 250 lux. Therefore, we calculated the signal segments' maximum value, and if either segment exceeded 250 lux, the outer surfaces of the front teeth were considered to be brushed in strong ambient light (ceiling light, sunlight). Considering variations in the maximum value of the brushing signal on the outer surfaces of the front teeth under different ambient light conditions, we compressed signals below a fixed value to ensure signal stability. When brushing the outer surfaces of the front teeth in dark or dim light conditions, both sensor signals' maximum values were around 150 lux. Therefore, to achieve consistency between brushing signals in strong light environments and dark or dim light environments, we used the following formula to compress the light intensity to below 150 lux while ensuring no changes in the minimum value and waveform of the signal:

$$x_{ALIC} = \frac{x - \min(x)}{max(x) - min(x)} \cdot (150 - min(x)) + min(x) \quad (5)$$

where x_{ALIC} is the corrected signal and x is the original signal. Figure 24 shows the corrected result of Figure 16.

6.3 Feature Extraction

Figure 25 shows the signals of 3 toothbrushing cycles of each Bass technique surface of a user in dim light. Next, we explain our analysis of feature extraction based on this figure. We found that the 2 sensor signals were significantly different for different brushing surfaces, so we extracted the following features of the two signals respectively.

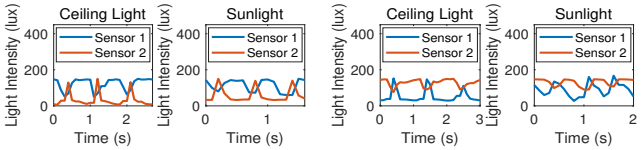

Fig. 24. Ambient light interference cancellation results of outer surfaces of (a) upper and (b) lower front teeth.

Independent features of the 2 sensor signals:

(1) Standard deviation: We found that when brushing the inner surfaces of the upper front teeth and the occlusal surfaces of molars, the range of light intensity received by the two sensors is relatively small because the angle between the sensor orientation and the brushing direction is small (30°) (Figure 7). In contrast, the signal variation range of the vertical stroke is large.

(2) Root mean square: We found that when brushing the inner surfaces of the upper molars, the 2 sensors received stronger light intensity than when brushing the outer surfaces of the upper molars. This is because when brushing the inner surfaces of the upper molars, the sensor is located in the mouth cavity and can receive the reflected light from the palate and tongue without the occlusion of the cheek. We are inspired by the calculation of the effective value of alternating current (i.e., root mean square). The root mean square can also represent the average light intensity level that swings up and down like the alternating current.

(3) Minimum value: if the sensor sticks close to the oral tissue at some time of brushing, it leads to a smaller minimum value, which is helpful to distinguish some surfaces. For example, when brushing the occlusal surfaces of the molars, the sensor on the outside of the molars and close to the cheek have a smaller minimum value.

(4) Maximum value: Similarly, the maximum value of the signal has a similar meaning.

Recall that user variability causes slight amplitude changes in the signal, which may weaken the effectiveness of features extracted from individual signals. To meet this challenge, we extracted the relatively stable relationship features between the 2 sensor signals.

Relationship features between 2 sensor signals:

(1) Root mean square difference: It reflects the relative position of the toothbrush in the oral cavity. For example, the sensor close to the cheek remains relatively weak when brushing the occlusal surfaces of molars because it is difficult for this sensor to receive reflected light. However, in a relatively open mouth, another sensor can receive reflected light from oral tissue (e.g., tongue, palate, and inner surfaces of the molars), so it continuously receives strong reflected light. This relatively stable spatial location relationship does not be affected by user variability. The positive and negative

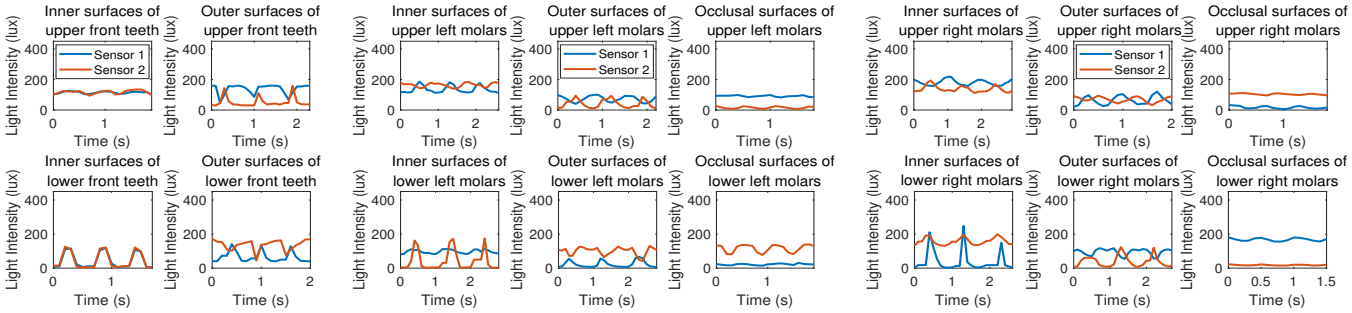

(a) Front teeth. (b) Left molars (c) Right molars

Fig. 25. A user's brushing signals on each Bass technique surface in dim light.

values generated by two sensors with different addresses are also helpful to distinguish left and right molars.

(2) Mean Euclidean distance: It measures the absolute similarity of the 2 sensor signals, which reflects the similarity of the oral structure on both two sides of the toothbrushes. The 2 sensor signals almost overlap when brushing the inner surface of the upper and lower front teeth because the left and right sensors of the toothbrush face similar oral structures. However, the oral structure on both sides of the toothbrush differs when brushing other surfaces. Taking the average can eliminate the influence of signal length (brushing speed).

(3) Cosine distance: We also calculated the cosine distance to measure the difference between the oral structures on both sides of the sensor, without being affected by light intensity.

(4) Pearson correlation coefficient: Correlation indicates whether the two sensors' changing trend of light intensity is consistent. For up-and-down strokes (except for the tongue's influence), the 2 sensors move in opposite directions, so their signals are negatively correlated. When brushing the inner surfaces of lower molars, the toothbrush sticks to the tongue when it is at the tooth's root. At this time, the received light of the downward sensor is weak, resulting in a positive signal correlation. The correlation between the 2 sensor signals is always stable for user variability.

Whenever we receive a signal for a toothbrushing cycle, we calculate the features and place them in the classifier. Note that our calculated features are not affected by signal length, and are immune to duration differences in user variability.

6.4 Classification

We standardized the 12 ($4 \times 2 + 4$) features extracted above using Z-score, changing the mean value of each feature to 1 and the standard deviation to 0. Then, we trained several classic classifiers, including Linear Discriminant Analysis (LDA), Weighted K-Nearest Neighbor (Weighted KNN), Support Vector Machine (SVM), Bagging Tree (BT), and Artificial Neural Networks (ANN) to identify the brushing surfaces. For Weighted KNN, we choose Euclidean distance as the distance metric and use an inverse square function as the weighting function with a k-value of 10. For the kernel function of SVM, we choose a linear function. The first layer size of the ANN is 100, the activation function is ReLU, and the number of fully connected layers is 1. After comparing the accuracy (Section 7.2.1), we chose to use Weighted KNN as the classifier for LiT.

7 SYSTEM EVALUATION

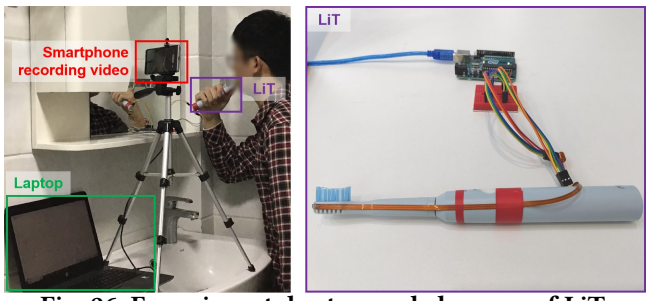

Fig. 26. Experimental setup and close-up of LiT.

7.1 Experimental Setup

We recruited 16 participants, including 6 women and 10 men; the age ranges from 21 to 46. They were first asked to watch the correct teaching video of toothbrushing [65] and carefully learn the correct Bass technique. Each participant used LiT (based on Abitelax F7 [69]) to brush his teeth 10 times, 2–4 minutes each time (Figure 26). The default condition is that the user stands still in front of the sink and brushes his/her teeth with Zendium^{TM} toothpaste (pea-sized amount) under the ceiling light and turns on the vibration. In addition, to further study the impact of other factors on LiT, in the evaluation of Section 7.3, 7.4 and 7.5, we required 6 users to brush their teeth 5 times under specified conditions, 2-4 minutes each time. We collected data under the framework of Figure 20 and inputted the collected data into the LiT algorithm. We used the leave-one-out to exclude the samples of users to be tested from the training set, and use the average value obtained by 10-fold cross-validation as the calculation result, in order to test the cross-user accuracy of LiT.

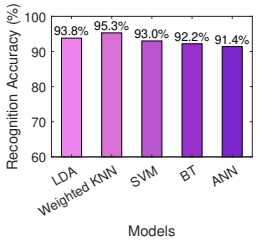

Fig. 27. Recognition accuracy of different models.

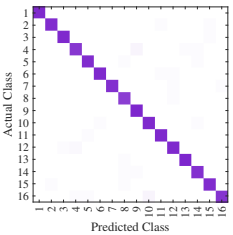

Fig. 28. Confusion matrix for 16 surfaces recognition.

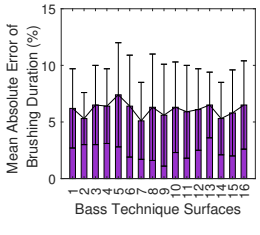

Fig. 29. Estimation error of duration of 16 surfaces.

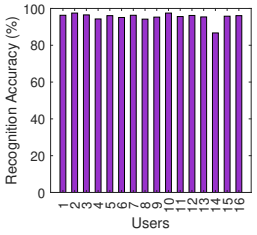

Fig. 30. Recognition accuracy across 16 users.

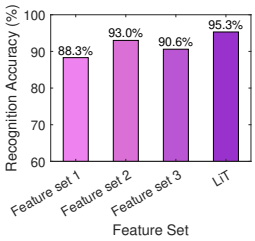

Fig. 31. Different feature sets accuracy.

7.2 Toothbrushing Monitoring Performance

7.2.1 Impact of the Model. As shown in Figure 27, all classifiers achieved over 90% recognition accuracy, with LDA and Weighted KNN exceeding 93%. The reason behind this may be that the feature dimensions we extracted are low and the features can be effectively distinguished. We chose Weighted KNN as it has the highest accuracy of 95.3%. Moreover, it has a good anti-noise ability and is insensitive to outliers compared with LDA.

7.2.2 Recognition Accuracy of Bass Technique Surfaces. The confusion matrix is shown in Figure 28. The recognition accuracy of LiT for each brushing surface is more than 87% and the average recognition accuracy is 95.3%, which indicates that the model of LiT training on other users can be generalized to other users. We believe we can "smooth" user variability by extracting stable features to reduce the data dimension. In particular, we extract stable relationships between 2 sensor signals to resist user variability.

7.2.3 Accuracy of Duration Estimation. Figure 29 shows the absolute error of estimation of brushing duration on each tooth surface, with an average error of 6.1%, indicating that periodic brushing signals can be accurately segmented using the periodicity and symmetry of periodic signals of brushing.

7.2.4 Impact of User Variability. Figure 30 shows the recognition accuracy of brushing surfaces of 16 users, ranging from 86.7% to 97.5%. Except for one user, the recognition accuracy of other users has exceeded 90%. We found that the lower accuracy of this user can be attributed to an impacted tooth affecting tooth flatness on the inner side of their upper right molars. Factors like wearing braces, impacted teeth or missing teeth can influence accuracy due to light reflection and transmission changes in the oral cavity. We recommend pre-training tailored models for users with unique oral structures.

7.2.5 Different Feature Sets. We also want to know which features are more effective for distinguishing the brushing surface. We compare the feature set used by LiT to three feature sets: (1) Feature set 1: Independent features of sensor 1 (4 features). (2) Feature set 2: Independent features of 2 sensor signals (8 features). (3) Feature set 3: The relationship features between 2 signals (4 features).

Figure 31 shows the results of this experiment. We found that the recognition accuracy of independent sensor signal features is relatively low (88.3%). The independent features of the 2 sensor signals can improve the recognition accuracy to 93.0%. This indicates that a single sensor has insufficient resolution, and the dual sensor design can help better distinguish brushing surfaces. The relationship features between 2 signals (only 4 features) achieve an accuracy of 90.6%, indicating that the relationship features between 2 signals can explain the physical significance behind and efficiently distinguish the brushing surface. The results of LiT with the highest recognition accuracy indicate that the combination of independent features and relationship features contribute to accurate and robust recognition of the brushing surfaces.

7.3 Robustness

We used the training model of 16 users by default to test the impact of environment and user movement on LiT and calculated the average recognition accuracy.

7.3.1 Impact of Toothbrush Vibration. The accuracy of surface recognition without vibration is 96.1%, which is only 0.84% higher than the accuracy with vibration (95.3%). Consistent with the analysis in Section 5.1, LiT works well with both manual toothbrushes and electric toothbrushes. The amplitude of the high-frequency vibration of the toothbrush is weak compared to the amplitude of the brush stroke, which is hardly reflected in the original signal with a low sampling rate of 10 Hz. In contrast, inertial sensor-based systems [6, 18–20] can only be used for manual toothbrushes because the vibrations from the toothbrush increase the drift error of the inertial sensors. The sound generated by brushing teeth can be masked by the vibration sound of the toothbrush vibro-motor, resulting in a microphone-based system [15–17] that can only be used with manual toothbrushes. MET [21] based on the vibro-motor magnetic field of the electric toothbrushes can only be used with electric toothbrushes.

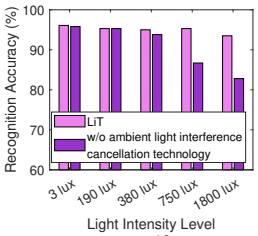

Fig. 32. Different light environments accuracy.

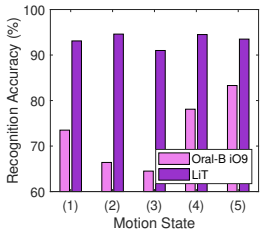

Fig. 33. Different user motion states accuracy.

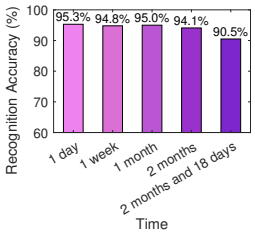

Fig. 34. Recognition accuracy over time.

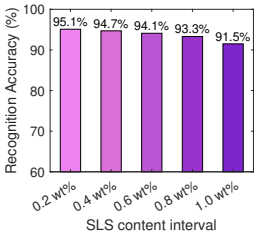

Fig. 35. Different training sample size accuracy.

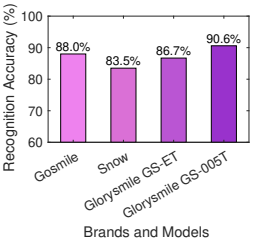

Fig. 36. Different toothbrushes accuracy.

7.3.2 Impact of Ambient light Interference. We tested the performance of LiT in 5 light environments: (1) Dark bathroom with 3 lux, simulating teeth brushing without turning on the light. (2) Morning bathroom with ceiling light off, 190 lux. (3) Balcony in natural light, 380 lux. (4) Nighttime bathroom with ceiling light on, around 750 lux. (5) Bathroom with ceiling light on a sunny afternoon, around 1,800 lux.

Figure 32 displays recognition accuracy for 5 scenarios, with and without ambient light interference cancellation. Even under strong ambient light ((4) and (5)), the recognition accuracy of LiT is more than 93.8%. However, without ambient light interference cancellation, accuracy drops to 82.8%. This is because when brushing most of the tooth surface, the toothbrush is located in the mouth and will not be affected by ambient light, but when brushing the outer surfaces of the front teeth, the sensor will receive strong ambient light. If the ambient light interference cancellation technology is not used, the amplitude and maximum value of one of the features will be affected. After using the ambient light interference elimination technology, the brushing signal on the outer surfaces of the front teeth returned to below 150 lux, ensuring the stability of the amplitude and maximum characteristics. To sum up, our proposed ambient light interference cancellation technology effectively enhances LiT's robustness to ambient light.

7.3.3 Impact of User Motion. Shielding user motion is one of our design goals. To examine the robustness of LiT to user motion, we introduced five kinds of potential user motion when brushing teeth: (1) Walking up and down in front of the sink when brushing. (2) Looking down at the video played on the mobile phone beside the sink when brushing. (3) From standing to sitting on a chair when brushing. (4) Putting the toothpaste back in its original position on the cabinet over the sink when brushing. (5) Rinsing non-brushing hands with water from the tap when brushing. Users used both LiT and the most advanced IMU-based Oral-B iO9 to brush their teeth under these five motion conditions.

The results in Figure 33 show that the recognition accuracy of LiT is 91.0%–94.6% when the users are in motion. This shows that user motion does not actually interfere with LiT. We believe this is because the toothbrush still maintains a relatively stable position in the oral cavity under the influence of various motions. In contrast, the recognition accuracy of Oral-B iO9 is only 64.5%–83.3% (Figure 33). This could be due to the principle of using integration to obtain absolute displacement and roll angle in IMU-based methods. The cumulative error in integration and the superposition of user motion on absolute displacement can easily lead to a decrease in recognition accuracy. Evidently, the sensing paradigm of LiT (sensing in the oral cavity) is very robust to user motion, which is also a unique advantage compared with existing technologies.

7.3.4 Temporal Stability. Abiterax F7 can last for 90 days under normal use [69]. Users may only charge the electric toothbrush once a month. We experimented to observe the accuracy of LiT during continuous operation. Figure 34 shows the recognition accuracy of 6 users over time. We found that the accuracy remained stable at around 95% over 2 months, with only a 6% drop in battery voltage and LED light intensity. This shows that LiT can run consistently for more than 2 months under the pre-training model without retraining the model. We believe that this temporal stability comes from the stability of the toothbrush's luminous model (the luminous properties after 2 months are still close to the measurement of Figure 4) and the stability of the user's oral structure. We found that after 2 months and 18 days of use, the voltage and LED light intensity dropped by 9% and the bristle ends were slightly worn, and the accuracy dropped to about 90%. Moreover, we found that the voltage decay was non-linear towards the end of use, dropping rapidly within three minutes from 3.3 V to below the vibration motor and LED drive threshold (2.9 V). Therefore, we believe that as long as the motor and LEDs can be driven, a maximum of 9% reduction in brightness will not significantly affect accuracy.

7.4 Generalization to Any Toothpaste

Toothpaste contains a surfactant, usually Sodium Lauryl Sulfate (SLS), with concentrations usually ranging from 0.5 wt% to 2.5 wt% [70], which helps create foam. For this study, we customized 11 toothpastes with SLS content ranging from

0.5 wt% to 2.5 wt% with 0.2 wt% intervals (each available in five different colors: white, red, yellow, blue, and green). Six users brushed their teeth five times with each toothpaste. Our findings show that the Weight KNN model's 10-fold cross-validation accuracy for toothpaste with varying colors but the same SLS content is approximately 94%. This might be because the expanded foam generated by SLS dilutes the pigment to a very light shade, still close to white. However, we found that the recognition accuracy of the brushing signals with high-foam toothpaste (2 wt% SLS) on the model trained with low-foam toothpaste (0.5% SLS) was 85.4%. This suggests that SLS content does affect recognition accuracy but also highlights the model's generalization capability.

We assume that users need to brush two specified tooth surfaces (the outer surface of the upper and lower left molars) for 10 s using their own toothpaste for initialization. LiT then calculates the sum of the weighted distances between the brushing signals and the 10 nearest samples of the same category in all pre-trained models and selects the model with the smallest distance as the classification model. To minimize pre-training costs, we explored the model's generalization ability. We randomly selected one brushing session signal from the five sessions of each user using the same toothpaste as the test set for that particular toothpaste. We utilized 4 other brushing sessions signal to train models for each SLS content, extracting model sets with 0.2 wt%, 0.4 wt%, 0.6 wt%, 0.8 wt%, and 1.0 wt% SLS intervals to simulate the desired training samples. For example, a model set with 0.8 wt% intervals includes 3 models with different SLS contents (0.9 wt%, 1.7 wt%, 2.5 wt%), meaning only these 3 SLS contents need to be trained. Then, we used the two 10-s specified brushing signals from each user's brushing session in the test set to select the corresponding models for each user's brushing session and calculated the average accuracy. Figure 35 is the relationship between SLS intervals and testing accuracy. To achieve balance, we recommend manufacturers to train 4 models with different SLS content at intervals of 0.6 wt% (0.7 wt%, 1.3 wt%, 1.9 wt%, 2.5 wt%) for each toothbrush model.

7.5 Extension to Other Toothbrushes

We also want to know whether the model we trained on Abitelax F7 can be used on other toothbrushes. Therefore, we have also tested 4 additional toothbrushes (GOSMILE, SNOW, Glorysmile GS-ET, and Glorysmile GS-005T). We found that the recognition accuracy of the 4 toothbrushes on the surface of Bass technique exceeded 83% without additional training (Figure 36). We found that different toothbrushes use different LEDs with different power. However, their luminous models are similar, that is, they can be regarded as a collection of point light sources with the same light intensity on the surface of an elliptical cylinder. We found that the difference between different types of toothbrushes is reflected in the amplitude change. However, the waveform of the 2 sensor signals and the relative position between them have not changed significantly.

8 CONCLUSION AND FUTURE WORK

LiT utilizes the toothbrush's light emission to monitor the brushing of 16 Bass technique surfaces. We established the oral cavity's light transmission model and found the proper photosensors deployment. We found the periodicity and symmetry features, designed the accurate brushing segmentation, and eliminated the impact of user variability by extracting stable and significant features. LiT has a recognition accuracy of up to 95.3% and a brushing duration estimation error of 6.1%, and maintains strong performance under various environmental disturbances and movement. However, some limitations should be addressed in the future as it is a proof-of-concept prototype.

From design: Current LiT attaches the sensor to the toothbrush head's surface. However, its protruding surface affects the user experience and is inconvenient to replace the toothbrush head. In the future, sensors can be integrated into the inner shell of the toothbrush head like the toothbrush LEDs.

Interactive paradigm: We plan to switch from wired data transmission to Bluetooth for real-time processing of light-intensity data on mobile devices. The mobile device will provide feedback on brushing and nursing advice using its touchscreen, speaker, or vibration features.

Combining with other sensors: Combining LiT with other sensors can enhance recognition and improve monitoring despite its usefulness in monitoring purposes alone.

Studies on larger populations: LiT may not cover the entire range of human diversity, so larger-scale studies are necessary to promote the deployment of LiT.

Enhancing generality: Our study is based on Bass technique since it is the most popular brushing method recommended by the ADA. Expansion of incorrect brushing identification and other brushing methods are the future work.

ACKNOWLEDGMENTS

This research was supported in part by China NSFC Grant U2001207, Guangdong Provincial Key Lab of Integrated Communication, Sensing and Computation for Ubiquitous Internet of Things, the Project of DEGP (No. 2021ZDZX1068).

ARTIFACT APPENDIX

The research artifacts accompanying this paper are available via https://doi.org/10.5281/zenodo.8260593.

REFERENCES

[1] Poul Erik Petersen. The world oral health report 2003: continuous improvement of oral health in the 21st century–the approach of the who global oral health programme. *Community Dentistry and oral epidemiology*, 31:3–24, 2003.

[2] Cherin C Pace and Gary H McCullough. The association between oral microorgansims and aspiration pneumonia in the institutionalized elderly: review and recommendations. *Dysphagia*, 25:307–322, 2010.

[3] Norman O Harris and Franklin Garcia-Godoy. *Primary preventive dentistry*. Upper Saddle River, NJ: Pearson Education, 2004.

[4] Iain LC Chapple, Fridus Van der Weijden, Christof Doerfer, David Herrera, Lior Shapira, David Polak, Phoebus Madianos, Anna Louropoulou, Eli Machtei, Nikos Donos, et al. Primary prevention of periodontitis: managing gingivitis. *Journal of clinical periodontology*, 42:S71–S76, 2015.

[5] Andrew Gallagher, Joseph Sowinski, James Bowman, Kathy Barrett, Shirley Lowe, Kartik Patel, Mary Lynn Bosma, and Jonathan E Creeth. The effect of brushing time and dentifrice on dental plaque removal in vivo. *American Dental Hygienists' Association*, 83(3):111–116, 2009.

[6] Sayma Akther, Nazir Saleheen, Mithun Saha, Vivek Shetty, and Santosh Kumar. mteeth: Identifying brushing teeth surfaces using wrist-worn inertial sensors. *Proceedings of the ACM on interactive, mobile, wearable and ubiquitous technologies*, 5(2):1–25, 2021.

[7] Renate Deinzer, Stefanie Ebel, Helen Blättermann, Ulrike Weik, and Jutta Margraf-Stiksrud. Toothbrushing: to the best of one's abilities is possibly not good enough. *BMC Oral Health*, 18:1–7, 2018.

[8] Tobias Winterfeld, N Schlueter, Daniela Harnacke, Jörg Illig, Jutta Margraf-Stiksrud, Renate Deinzer, and Carolina Ganss. Toothbrushing and flossing behaviour in young adults—a video observation. *Clinical oral investigations*, 19:851–858, 2015.

[9] Gudrun Sangnes and Per Gjermo. Prevalence of oral soft and hard tissue lesions related to mechanical toothcleansing procedures. *Community Dentistry and Oral Epidemiology*, 4(2):77–83, 1976.

[10] Sara Cioccari Oliveira, Dagmar Else Slot, and Fridus van der Weijden. Is it safe to use a toothbrush? *Acta Odontologica Scandinavica*, 72(8):561–569, 2014.

[11] Adrian U Yap. Oral health equals total health: A brief review. *Journal of Dentistry Indonesia*, 24(2):59–62, 2017.

[12] Yu-Chen Chang, Jin-Ling Lo, Chao-Ju Huang, Nan-Yi Hsu, Hao-Hua Chu, Hsin-Yen Wang, Pei-Yu Chi, and Ya-Lin Hsieh. Playful toothbrush: ubicomp technology for teaching tooth brushing to kindergarten children. In *Proceedings of the SIGCHI conference on human factors in computing systems*, pages 363–372, 2008.

[13] Nahyeon Lee, Doyoung Jang, Yeji Kim, Byung-Cull Bae, and Jun-Dong Cho. Denteach: A device for fostering children's good tooth-brushing habits. In *Proceedings of the The 15th International Conference on Interaction Design and Children*, pages 619–624, 2016.

[14] Marco Marcon, Augusto Sarti, and Stefano Tubaro. Toothbrush motion analysis to help children learn proper tooth brushing. *Computer Vision and Image Understanding*, 148:34–45, 2016.

[15] Zhenchao Ouyang, Jingfeng Hu, Jianwei Niu, and Zhiping Qi. An asymmetrical acoustic field detection system for daily tooth brushing monitoring. In *GLOBECOM 2017-2017 IEEE Global Communications Conference*, pages 1–6. IEEE, 2017.

[16] Jay Prakash, Zhijian Yang, Yu-Lin Wei, Haitham Hassanieh, and Romit Roy Choudhury. Earsense: earphones as a teeth activity sensor. In *Proceedings of the 26th Annual International Conference on Mobile Computing and Networking*, pages 1–13, 2020.

[17] Joseph Korpela, Ryosuke Miyaji, Takuya Maekawa, Kazunori Nozaki, and Hiroo Tamagawa. Evaluating tooth brushing performance with smartphone sound data. In *Proceedings of the 2015 ACM International Joint Conference on Pervasive and Ubiquitous Computing*, pages 109–120, 2015.

[18] Young-Jae Lee, Pil-Jae Lee, Kyeong-Seop Kim, Wonse Park, Kee-Deog Kim, Dosik Hwang, and Jeong-Whan Lee. Toothbrushing region detection using three-axis accelerometer and magnetic sensor. *IEEE Transactions on Biomedical Engineering*, 59(3):872–881, 2011.

[19] Hua Huang and Shan Lin. Toothbrushing monitoring using wrist watch. In *Proceedings of the 14th ACM Conference on Embedded Network Sensor Systems CD-ROM*, pages 202–215, 2016.

[20] Chengwen Luo, Xingyu Feng, Junliang Chen, Jianqiang Li, Weitao Xu, Wei Li, Li Zhang, Zahir Tari, and Albert Y Zomaya. Brush like a dentist: Accurate monitoring of toothbrushing via wrist-worn gesture sensing. In *IEEE INFOCOM 2019-IEEE Conference on Computer Communications*, pages 1234–1242. IEEE, 2019.

[21] Hua Huang and Shan Lin. Met: a magneto-inductive sensing based electric toothbrushing monitoring system. In *Proceedings of the 26th Annual International Conference on Mobile Computing and Networking*, pages 1–14, 2020.

[22] Elina A Genina, Vladimir A Titorenko, Andrey V Belikov, Alexey N Bashkatov, and Valery V Tuchin. Adjunctive dental therapy via tooth plaque reduction and gingivitis treatment by blue light-emitting diodes tooth brushing. *Journal of Biomedical Optics*, 20(12):128004–128004, 2015.

[23] Nadja Bjurshammar, Sebastian Malmqvist, Gunnar Johannsen, Elisabeth Boström, Jonas Fyrestam, Conny Östman, Annsofi Johannsen, et al. Effects of adjunctive daily blue light toothbrushing on dental plaque and gingival inflammation—a randomized controlled study. *Open Journal of Stomatology*, 8(10):287, 2018.

[24] Si-Mook Kang, Hoi-In Jung, and Baek-Il Kim. Susceptibility of oral bacteria to antibacterial photodynamic therapy. *Journal of oral microbiology*, 11(1):1644111, 2019.

[25] Anaga Ojo, Samir Chatterjee, Harold W Neighbors, Gretchen A Piatt, Sanjoy Moulik, Bonita D Neighbors, Jamie Abelson, Chris Krenz, and Darlene Jones. Oh-buddy: mobile phone texting based intervention for diabetes and oral health management. In *2015 48th Hawaii International Conference on System Sciences*, pages 803–813. IEEE, 2015.

[26] Harish C Jadhav, Arun S Dodamani, GN Karibasappa, Rahul G Naik, Mahesh R Khairnar, Manjiri A Deshmukh, and Prashanth Vishwakarma. Effect of reinforcement of oral health education message through short messaging service in mobile phones: a quasi-experimental trial. *International journal of telemedicine and applications*, 2016:2–2, 2016.

[27] Kee-Deog Kim, Jin-Sun Jeong, Hae Na Lee, Yu Gu, Kyeong-Seop Kim, Jeong-Whan Lee, and Wonse Park. Efficacy of computer-assisted, 3d motion-capture toothbrushing instruction. *Clinical oral investigations*, 19:1389–1394, 2015.

[28] Tatsuo Nakajima, Vili Lehdonvirta, Eiji Tokunaga, and Hiroaki Kimura. Reflecting human behavior to motivate desirable lifestyle. In *Proceedings of the 7th ACM conference on Designing interactive systems*, pages 405–414, 2008.

[29] Yuan Liang, Hsuan Wei Fan, Zhujun Fang, Leiying Miao, Wen Li, Xuan Zhang, Weibin Sun, Kun Wang, Lei He, and Xiang'Anthony' Chen. Oralcam: enabling self-examination and awareness of oral health using a smartphone camera. In *Proceedings of the 2020 CHI conference on human factors in computing systems*, pages 1–13, 2020.

[30] Guy Tobias, Assaf B Spanier, et al. Developing a mobile app (igam) to promote gingival health by professional monitoring of dental selfies: user-centered design approach. *JMIR mHealth and uHealth*, 8(8):e19433, 2020.

[31] Sayma Akther, Nazir Saleheen, Shahin Alan Samiei, Vivek Shetty, Emre Ertin, and Santosh Kumar. moral: An mhealth model for inferring oral hygiene behaviors in-the-wild using wrist-worn inertial sensors.

Proceedings of the ACM on Interactive, Mobile, Wearable and Ubiquitous Technologies, 3(1):1–25, 2019.

[32] Muhammad Fahim, Vishal Sharma, and Trung Q Duong. A wearable-based preventive model to promote oral health through personalized notification. In *2022 44th Annual International Conference of the IEEE Engineering in Medicine & Biology Society (EMBC)*, pages 4282–4285. IEEE, 2022.

[33] Takuma Yoshitani, Masa Ogata, and Koji Yatani. Lumio: a plaque-aware toothbrush. In *Proceedings of the 2016 ACM International Joint Conference on Pervasive and Ubiquitous Computing*, pages 605–615, 2016.

[34] Ana Caraban, Maria José Ferreira, Rúben Gouveia, and Evangelos Karapanos. Social toothbrush: fostering family nudging around tooth brushing habits. In *Adjunct proceedings of the 2015 acm international joint conference on pervasive and ubiquitous computing and proceedings of the 2015 acm international symposium on wearable computers*, pages 649–653, 2015.

[35] Kaixin Chen, Yongzhi Huang, Yicong Chen, Haobin Zhong, Lihua Lin, Lu Wang, and Kaishun Wu. Lisee: A headphone that provides all-day assistance for blind and low-vision users to reach surrounding objects. *Proceedings of the ACM on Interactive, Mobile, Wearable and Ubiquitous Technologies*, 6(3):1–30, 2022.

[36] Tobias Röddiger, Christopher Clarke, Paula Breitling, Tim Schneegans, Haibin Zhao, Hans Gellersen, and Michael Beigl. Sensing with earables: A systematic literature review and taxonomy of phenomena. *Proceedings of the ACM on Interactive, Mobile, Wearable and Ubiquitous Technologies*, 6(3):1–57, 2022.

[37] Zhijian Yang, Yu-Lin Wei, Sheng Shen, and Romit Roy Choudhury. Ear-ar: indoor acoustic augmented reality on earphones. In *Proceedings of the 26th Annual International Conference on Mobile Computing and Networking*, pages 1–14, 2020.

[38] Xieyang Xu, Yang Shen, Junrui Yang, Chenren Xu, Guobin Shen, Guojun Chen, and Yunzhe Ni. Passivevlc: Enabling practical visible light backscatter communication for battery-free iot applications. In *Proceedings of the 23rd Annual International Conference on Mobile Computing and Networking*, pages 180–192, 2017.

[39] Minhao Cui, Qing Wang, and Jie Xiong. Radioinlight: doubling the data rate of vlc systems. In *Proceedings of the 27th Annual International Conference on Mobile Computing and Networking*, pages 615–627, 2021.

[40] Chi Lin, Yongda Yu, Jie Xiong, Yichuan Zhang, Lei Wang, Guowei Wu, and Zhongxuan Luo. Shrimp: a robust underwater visible light communication system. In *Proceedings of the 27th Annual International Conference on Mobile Computing and Networking*, pages 134–146, 2021.

[41] Zhao Tian, Kevin Wright, and Xia Zhou. The darklight rises: Visible light communication in the dark. In *Proceedings of the 22nd Annual International Conference on Mobile Computing and Networking*, pages 2–15, 2016.

[42] Song Liu and Tian He. Smartlight: Light-weight 3d indoor localization using a single led lamp. In *Proceedings of the 15th ACM Conference on Embedded Network Sensor Systems*, pages 1–14, 2017.

[43] Chi Zhang and Xinyu Zhang. Litell: Robust indoor localization using unmodified light fixtures. In *Proceedings of the 22nd Annual International Conference on Mobile Computing and Networking*, pages 230–242, 2016.

[44] Chi Zhang and Xinyu Zhang. Pulsar: Towards ubiquitous visible light localization. In *Proceedings of the 23rd Annual International Conference on Mobile Computing and Networking*, pages 208–221, 2017.

[45] Tianxing Li, Chuankai An, Zhao Tian, Andrew T Campbell, and Xia Zhou. Human sensing using visible light communication. In *Proceedings of the 21st Annual International Conference on Mobile Computing and Networking*, pages 331–344, 2015.

[46] Tianxing Li, Qiang Liu, and Xia Zhou. Practical human sensing in the light. In *Proceedings of the 14th Annual International Conference on Mobile Systems, Applications, and Services*, pages 71–84, 2016.

[47] Raghav H Venkatnarayan and Muhammad Shahzad. Gesture recognition using ambient light. *Proceedings of the ACM on Interactive, Mobile, Wearable and Ubiquitous Technologies*, 2(1):1–28, 2018.

[48] Zimo Liao, Zhicheng Luo, Qianyi Huang, Linfeng Zhang, Fan Wu, Qian Zhang, and Yi Wang. Smart: screen-based gesture recognition on commodity mobile devices. In *Proceedings of the 27th Annual International Conference on Mobile Computing and Networking*, pages 283–295, 2021.

[49] Dong Ma, Guohao Lan, Mahbub Hassan, Wen Hu, Mushfika B Upama, Ashraf Uddin, and Moustafa Youssef. Solargest: Ubiquitous and battery-free gesture recognition using solar cells. In *The 25th annual international conference on mobile computing and networking*, pages 1–15, 2019.

[50] Chi Zhang, Josh Tabor, Jialiang Zhang, and Xinyu Zhang. Extending mobile interaction through near-field visible light sensing. In *Proceedings of the 21st Annual International Conference on Mobile Computing and Networking*, pages 345–357, 2015.

[51] Song Liu and Tian He. Bitlight: Turning dlp projections into an interactive surface through bit-level light encoding. *Proceedings of the ACM on Interactive, Mobile, Wearable and Ubiquitous Technologies*, 4(4):1–23, 2020.

[52] Hangcheng Cao, Daibo Liu, Hongbo Jiang, Ruize Wang, Zhe Chen, and Jie Xiong. Lipauth: Hand-dependent light intensity patterns for resilient user authentication. *ACM Transactions on Sensor Networks*, 2022.

[53] Yongzhi Huang, Kaixin Chen, Lu Wang, Yinying Dong, Qianyi Huang, and Kaishun Wu. Lili: liquor quality monitoring based on light signals. In *Proceedings of the 27th Annual International Conference on Mobile Computing and Networking*, pages 256–268, 2021.

[54] Yongzhi Huang, Kaixin Chen, Jiayi Zhao, Lu Wang, and Kaishun Wu. Beverage deterioration monitoring based on surface tension dynamics and absorption spectrum analysis. *IEEE Transactions on Mobile Computing*, 2023.

[55] Tauhidur Rahman, Alexander T Adams, Perry Schein, Aadhar Jain, David Erickson, and Tanzeem Choudhury. Nutrilyzer: A mobile system for characterizing liquid food with photoacoustic effect. In *Proceedings of the 14th ACM Conference on Embedded Network Sensor Systems CD-ROM*, pages 123–136, 2016.

[56] Haiyan Hu, Qianyi Huang, and Qian Zhang. Babynutri: A cost-effective baby food macronutrients analyzer based on spectral reconstruction. *Proceedings of the ACM on Interactive, Mobile, Wearable and Ubiquitous Technologies*, 7(1):1–30, 2023.

[57] Tianming Zhao, Yan Wang, Jian Liu, Jerry Cheng, Yingying Chen, and Jiadi Yu. Robust continuous authentication using cardiac biometrics from wrist-worn wearables. *IEEE Internet of Things Journal*, 9(12):9542–9556, 2021.

[58] Fei Gao, Qiwen Peng, Xiaohua Feng, Bo Gao, and Yuanjin Zheng. Single-wavelength blood oxygen saturation sensing with combined optical absorption and scattering. *IEEE Sensors Journal*, 16(7):1943–1948, 2015.

[59] Nam Bui, Nhat Pham, Jessica Jacqueline Barnitz, Zhanan Zou, Phuc Nguyen, Hoang Truong, Taeho Kim, Nicholas Farrow, Anh Nguyen, Jianliang Xiao, et al. ebp: A wearable system for frequent and comfortable blood pressure monitoring from user's ear. In *The 25th annual international conference on mobile computing and networking*, pages 1–17, 2019.

[60] Yetong Cao, Huijie Chen, Fan Li, and Yu Wang. Crisp-bp: Continuous wrist ppg-based blood pressure measurement. In *Proceedings of the 27th Annual International Conference on Mobile Computing and Networking*,

pages 378–391, 2021.

[61] Tianming Zhao, Yan Wang, Jian Liu, and Yingying Chen. Your heart won't lie: Ppg-based continuous authentication on wrist-worn wearable devices. In *Proceedings of the 24th Annual International Conference on Mobile Computing and Networking*, pages 783–785, 2018.

[62] Takahiro Hashizume, Takuya Arizono, and Koji Yatani. Auth 'n'scan: Opportunistic photoplethysmography in mobile fingerprint authentication. *Proceedings of the ACM on Interactive, Mobile, Wearable and Ubiquitous Technologies*, 1(4):1–27, 2018.

[63] Ada. brushing your teeth. https://www.mouthhealthy.org/-/media/project/ada-organization/ada/mouthhealthy/files/activity-sheets/adahowtobrush_eng.pdf, 2023.

[64] Ada. prevention and education. https://www.ada.org/advocacy/prevention-and-education, 2023.

[65] Clínica médico dental pardiñas. tooth brushing – how to brush your teeth. https://www.youtube.com/watch?v=olsUdRrYY70, 2023.

[66] Wikidoc. tooth brushing. https://www.wikidoc.org/index.php/Tooth_brushing, 2023.

[67] Joseph M Kahn and John R Barry. Wireless infrared communications. *Proceedings of the IEEE*, 85(2):265–298, 1997.

[68] Zabih Ghassemlooy, Wasiu Popoola, and Sujan Rajbhandari. *Optical wireless communications: system and channel modelling with Matlab®*. CRC press, 2019.

[69] Abitelax. f7 blue light sterilization electric toothbrush. https://www.moboplus.hk/product/669869, 2023.

[70] Frank Lippert. An introduction to toothpaste-its purpose, history and ingredients. In *Toothpastes*, volume 23, pages 1–14. Karger Publishers, 2013.